Geology and mineralogy of the Auki Crater, Tyrrhena Terra, Mars: A possible post impact-induced hydrothermal system

CARROZZO, F. Giacomo[1]
G. Di Achille[2], F. Salese[3], F. Altieri[1], G. Bellucci[1]

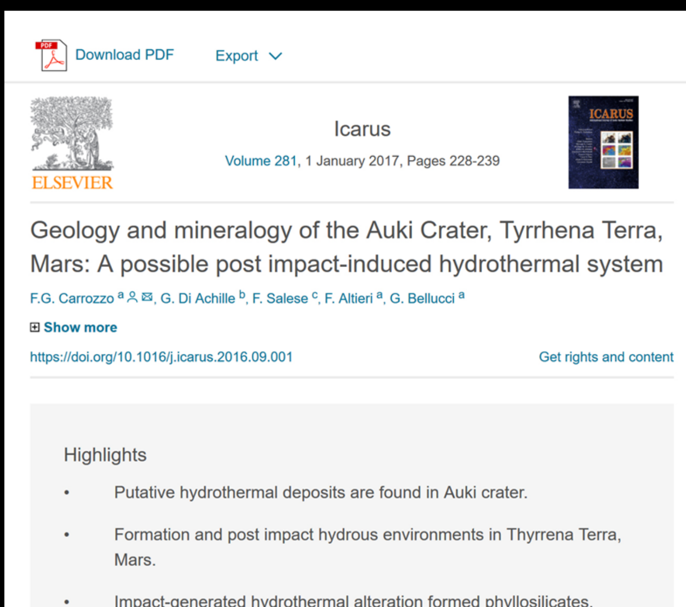
Download PDF Export

Icarus
Volume 281, 1 January 2017, Pages 228-239

Geology and mineralogy of the Auki Crater, Tyrrhena Terra, Mars: A possible post impact-induced hydrothermal system

F.G. Carrozzo [a], G. Di Achille [b], F. Salese [c], F. Altieri [a], G. Bellucci [a]

Show more

https://doi.org/10.1016/j.icarus.2016.09.001

Get rights and content

Highlights

- Putative hydrothermal deposits are found in Auki crater.
- Formation and post impact hydrous environments in Thyrrena Terra, Mars.
- Impact-generated hydrothermal alteration formed phyllosilicates,

a *Istituto di Astrofisica e Planetologia Spaziali, INAF, Rome, Italy*
b *Osservatorio Astronomico di Teramo, INAF, Teramo, Italy*
c *International Research School of Planetary Sciences, Pescara, Italy*

giacomo.carrozzo@iaps.inaf.it

LOCATION OF THE AUKI CRATER

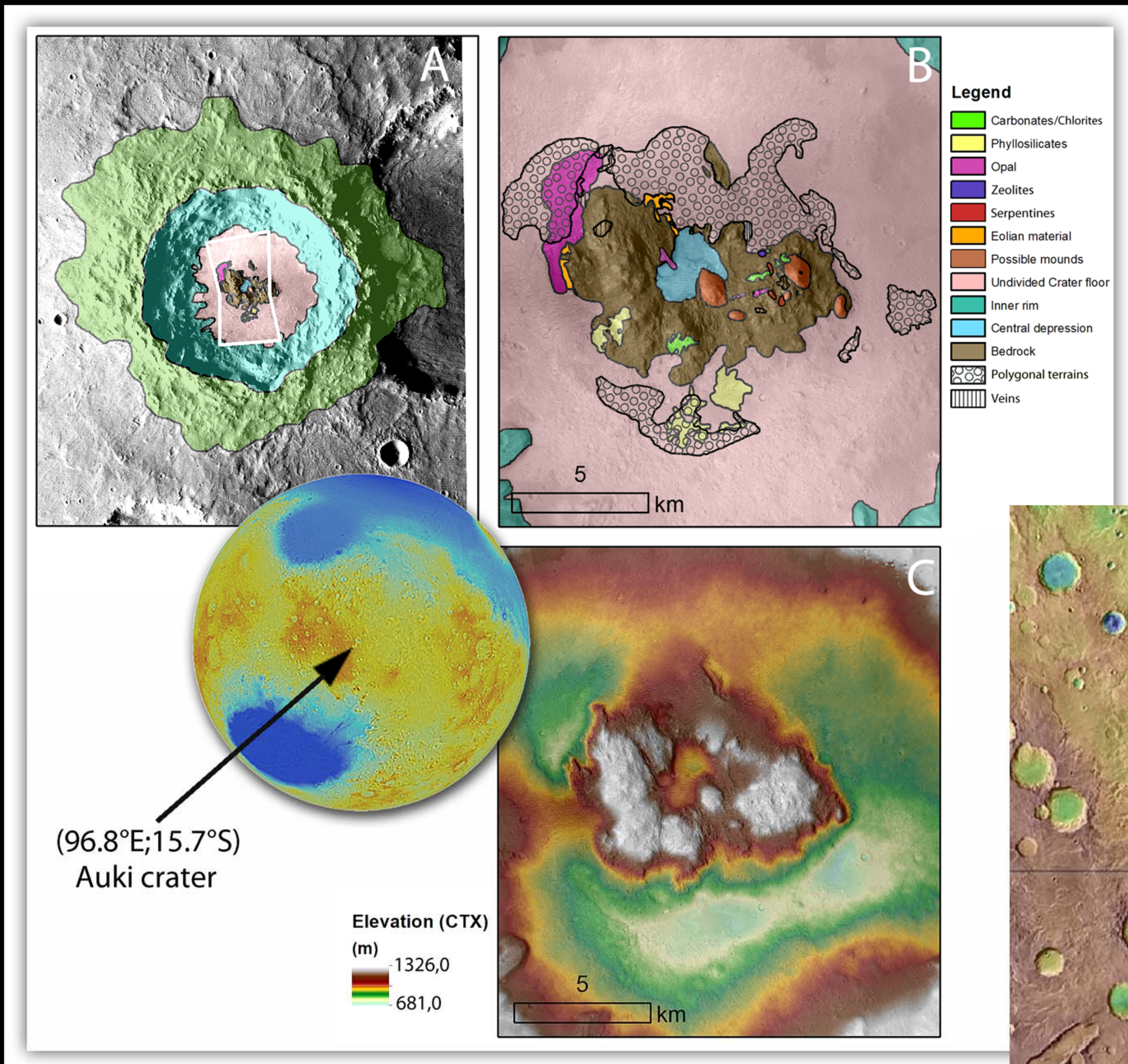

Location map of the Auki Crater (globe) and overall geomorphologic map of the crater showing (A) the footprint of the CRISM observation; (B) close-up of the geomorphological map for the central peak pit; (C) stereo-derived topography of the same region as figure B.
It is 38 km in dimeter located in Tyrrhena Terra.

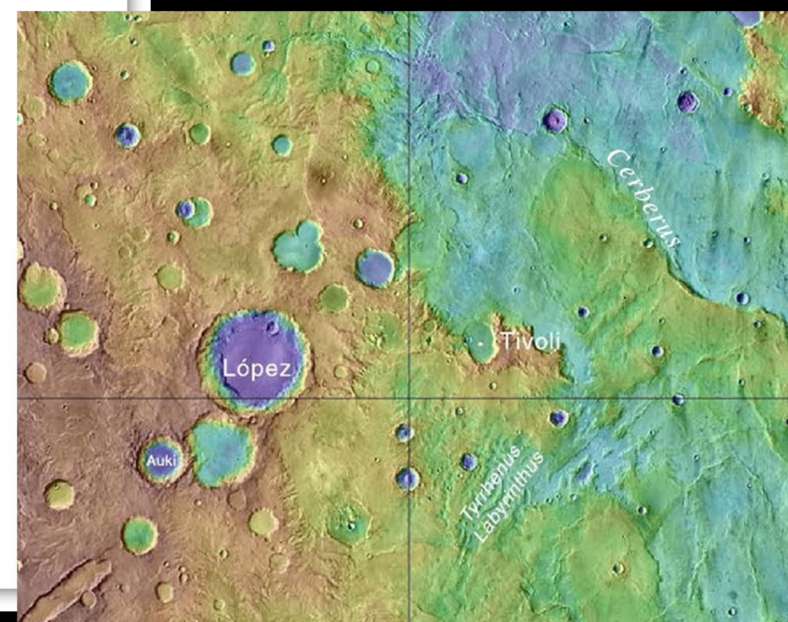

SCHEMATIC CROSS SECTION OF A COMPLEX CRATER

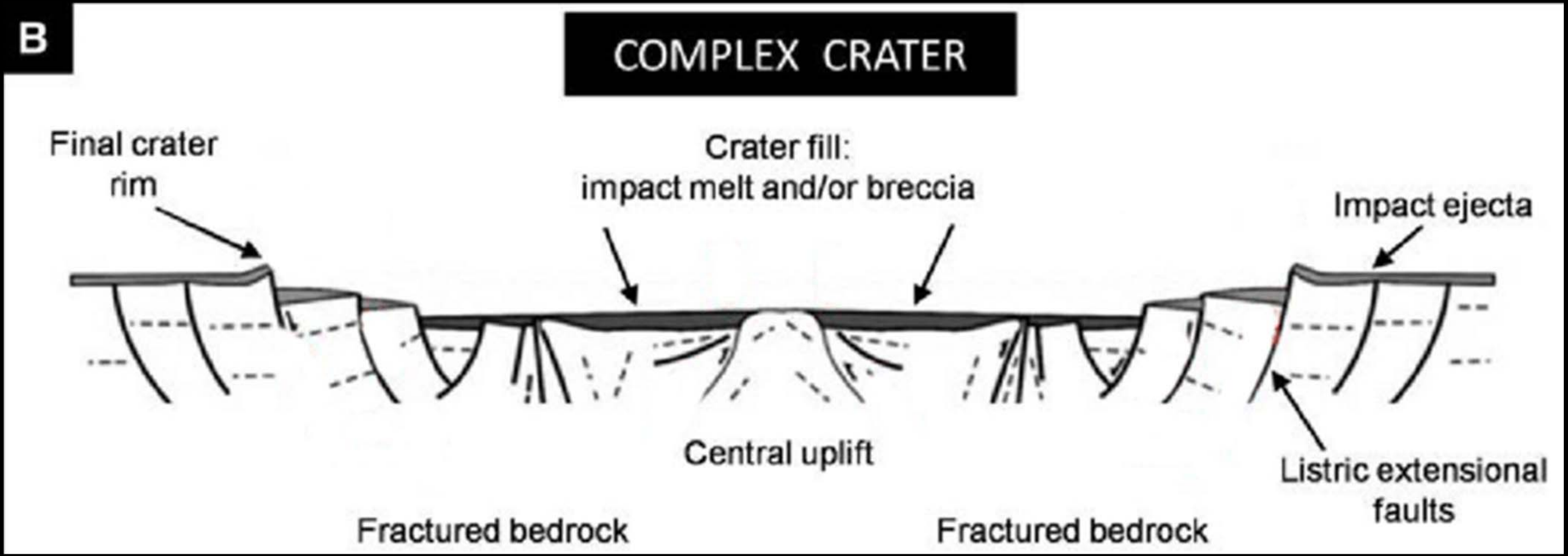

Schematic cross section of a generic impact crater complex (Oehler and Etiope, 2017). Complex crater adapted from Melosh (1989) and Osinski et al. (2005);

Two main high T locations:

- Melt sheet in the crater cavity
- Central uplift

The interaction of water with hot materials forms a hot rock-water circulatory system that can dissolve, transport, and precipitate various mineral species, resulting in characteristic hydrothermal mineral alteration assemblage. Alteration minerals are important indicators of the thermochemical environment at the time of their formation.

SCHEMATIC CROSS SECTION OF A COMPLEX CRATER

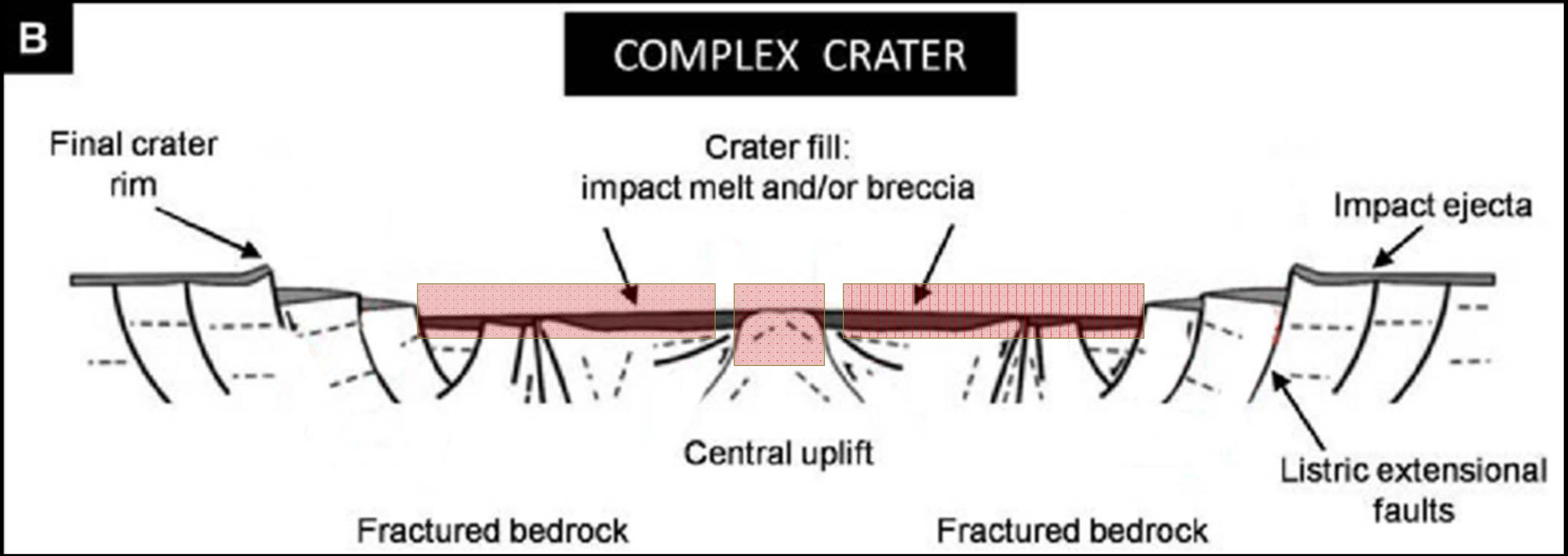

Schematic cross section of a generic impact crater complex (Oehler and Etiope, 2017). Complex crater adapted from Melosh (1989) and Osinski et al. (2005);

Two main high T locations:

- Melt sheet in the crater cavity
- Central uplift

Alteration minerals are important indicators of the thermochemical environment at the time of their formation. The interaction of water with hot materials forms a hot rock-water circulatory system that can dissolve, transport, and precipitate various mineral species, resulting in characteristic hydrothermal mineral alteration assemblage

SCHEMATIC CROSS SECTION OF A COMPLEX CRATER

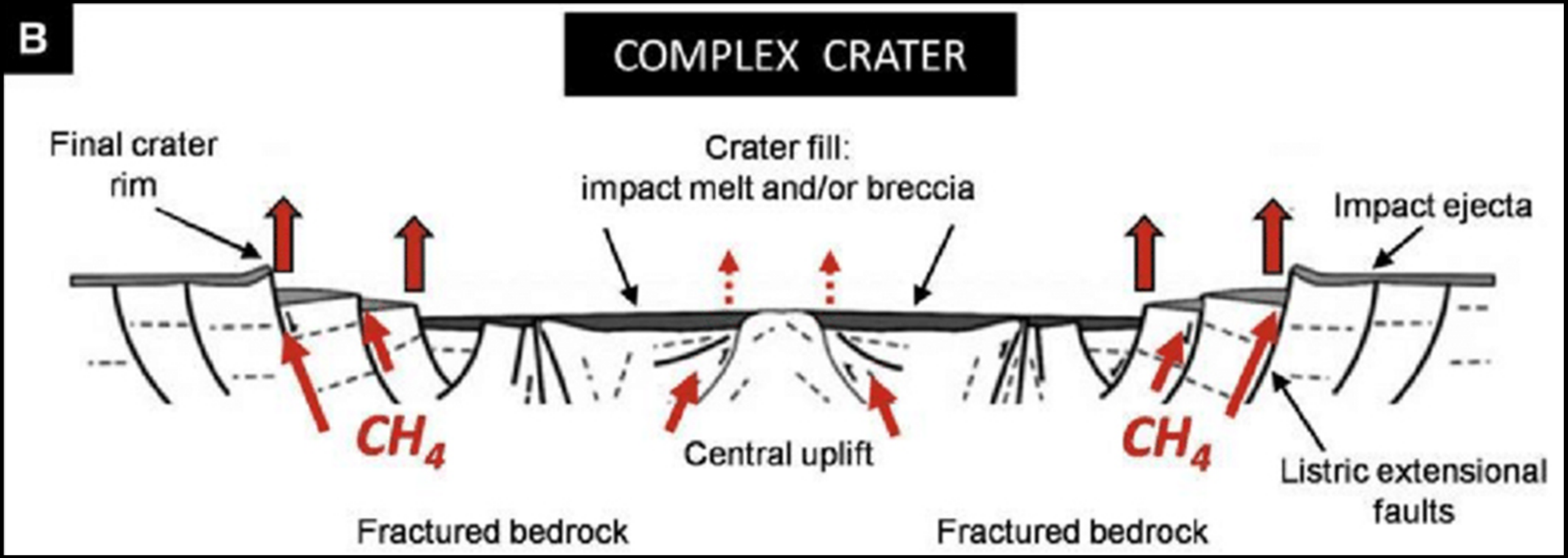

Schematic cross sections of impact craters. These illustrate potential CH 4 generated at depth (by any process) and subsequent fluid flow (arrows) through fractures, faults, and unconformity surfaces. Complex crater, adapted from Melosh (1989) and Osinski et al. (2005); dashed arrow indicates potential CH 4 release associated with central uplifts.

Methane generated in the subsurface could be stored in fractures, zeolite and mud volcanos like mounds (Oehler and Etiope, 2017).

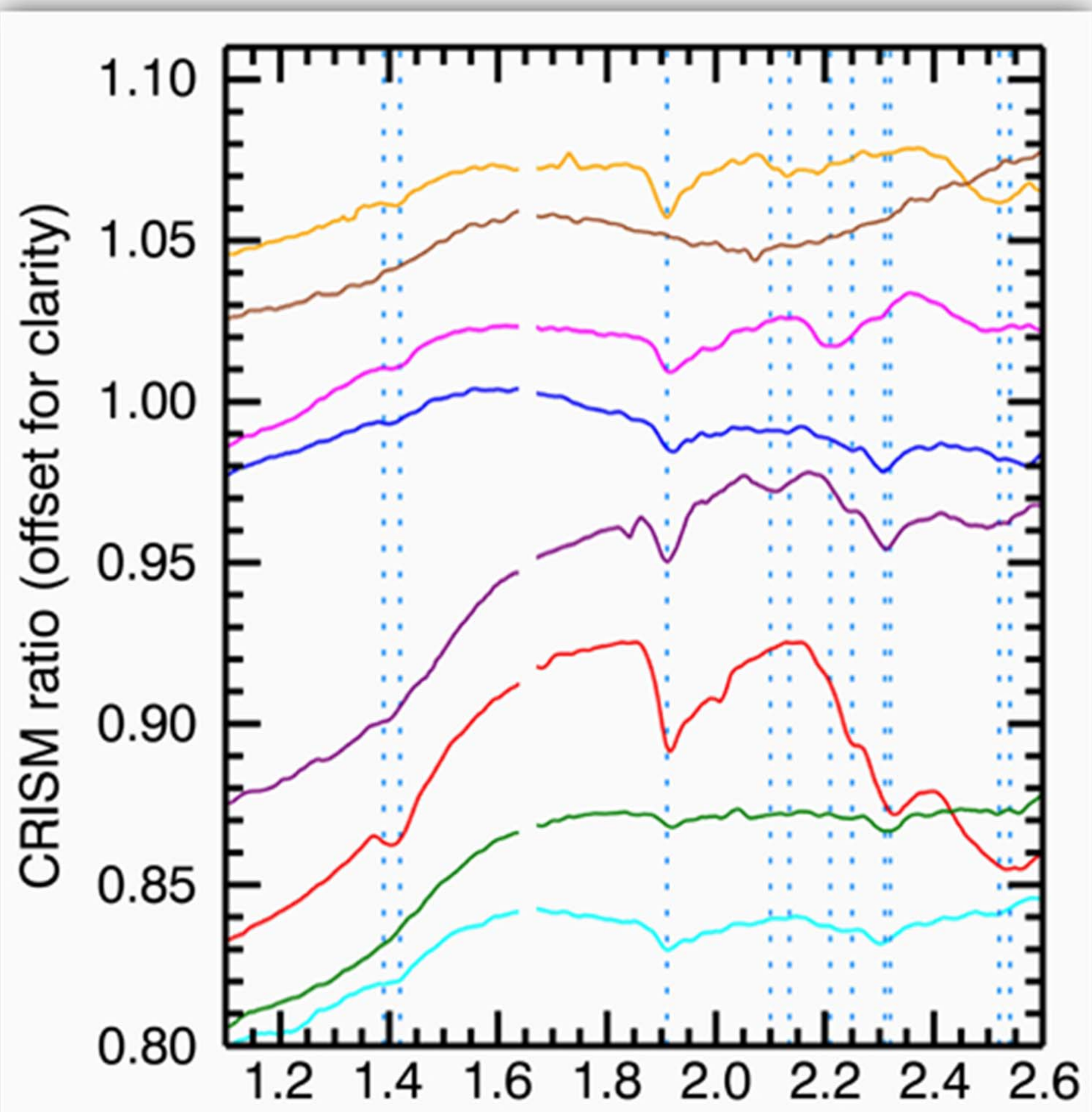

CRISM ratio (offset for clarity)
1.10
1.05
1.00
0.95
0.90
0.85
0.80
1.2
1.4
1.6
1.8
2.0
2.2
2.4
2.6

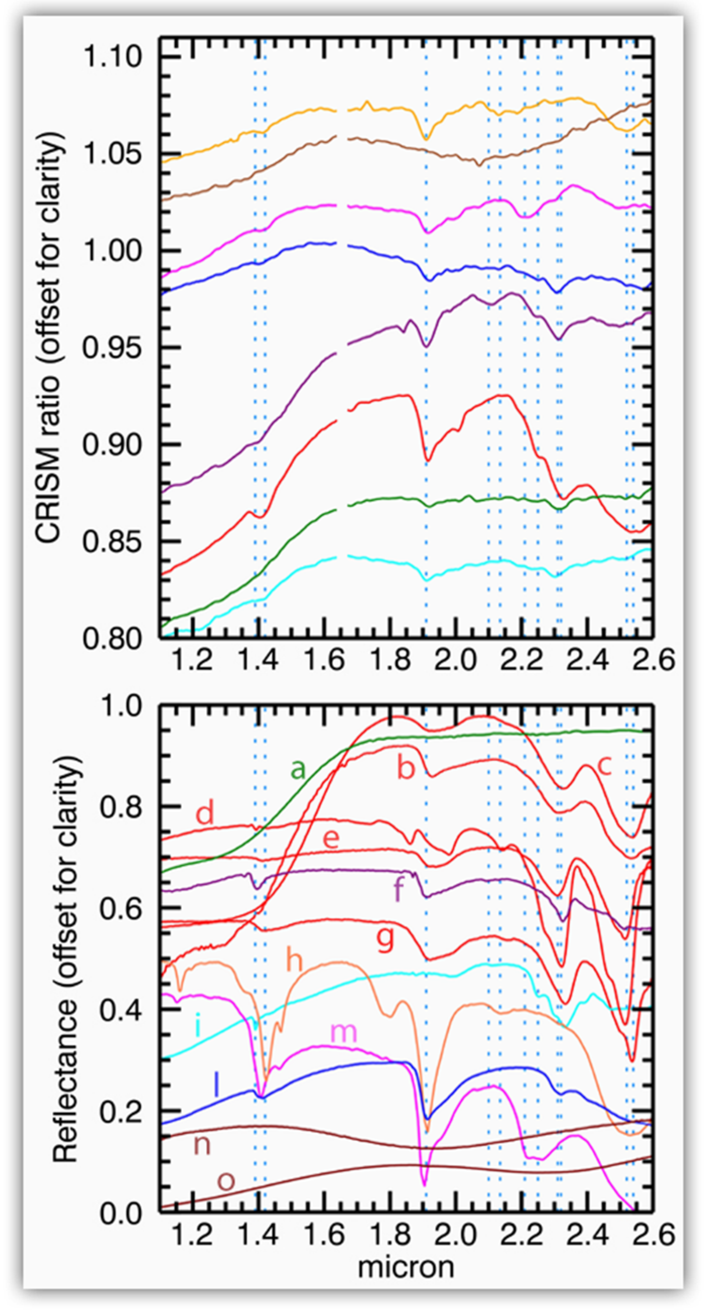

CRISM spectra ratio (top panel) compared to various library spectra (bottom panel). Olivine is in green color (a-olivine), carbonate in red (b-siderite, c-ankerite, d-calcite, e-calcite, g-dolomite), serpentine in purple (f-serpentine), zeolites in orange (h-analcime), chlorites in cyan (i-chlorite), smectite in blue (l-saponite), silica in magenta (m-opal), pyroxene in maroon (n-LCP, o-HCP).

To identify the minerals, we compare the spectral signatures of the ratioed spectra with the spectra of the ASTER (Baldrige et al., 2009), CRISM (Murchie et al., 2007), USGS (Clark et al., 2007) and RELAB spectral libraries.

CENTRAL UPLIFT

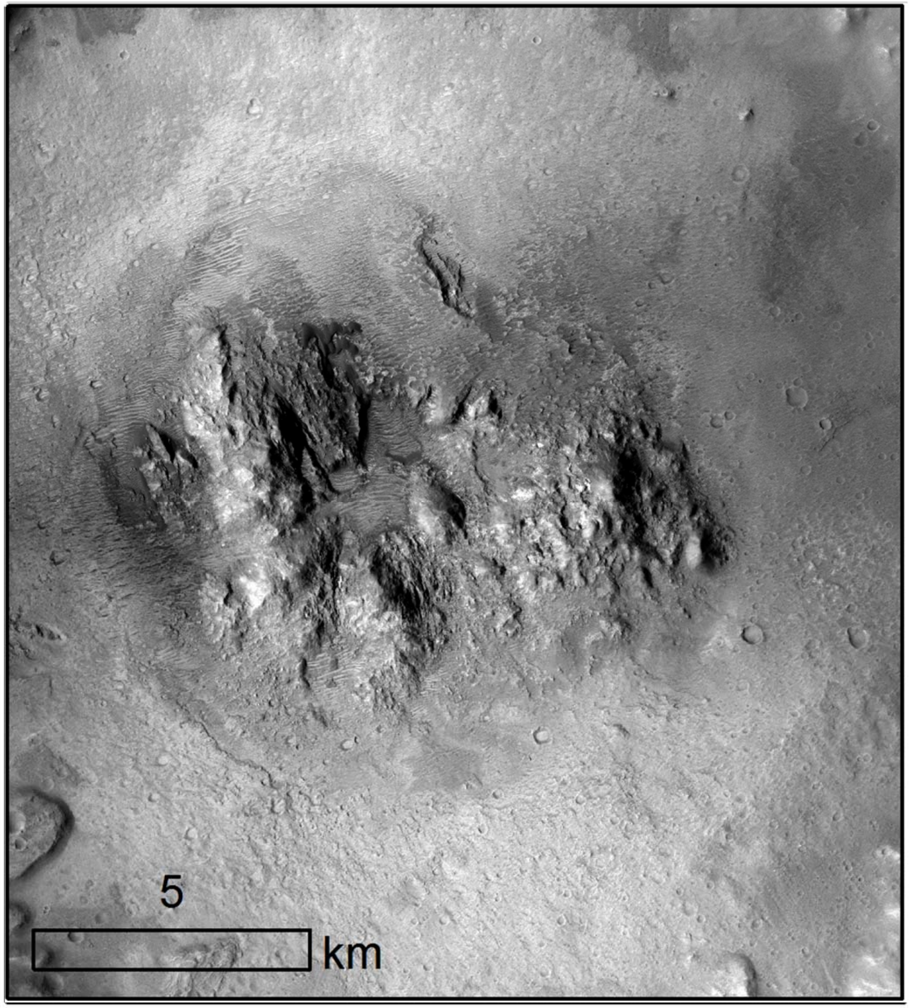

LEGEND

A) distribution of the most representative minerals and (B) close-up of the central peak pit of panel A

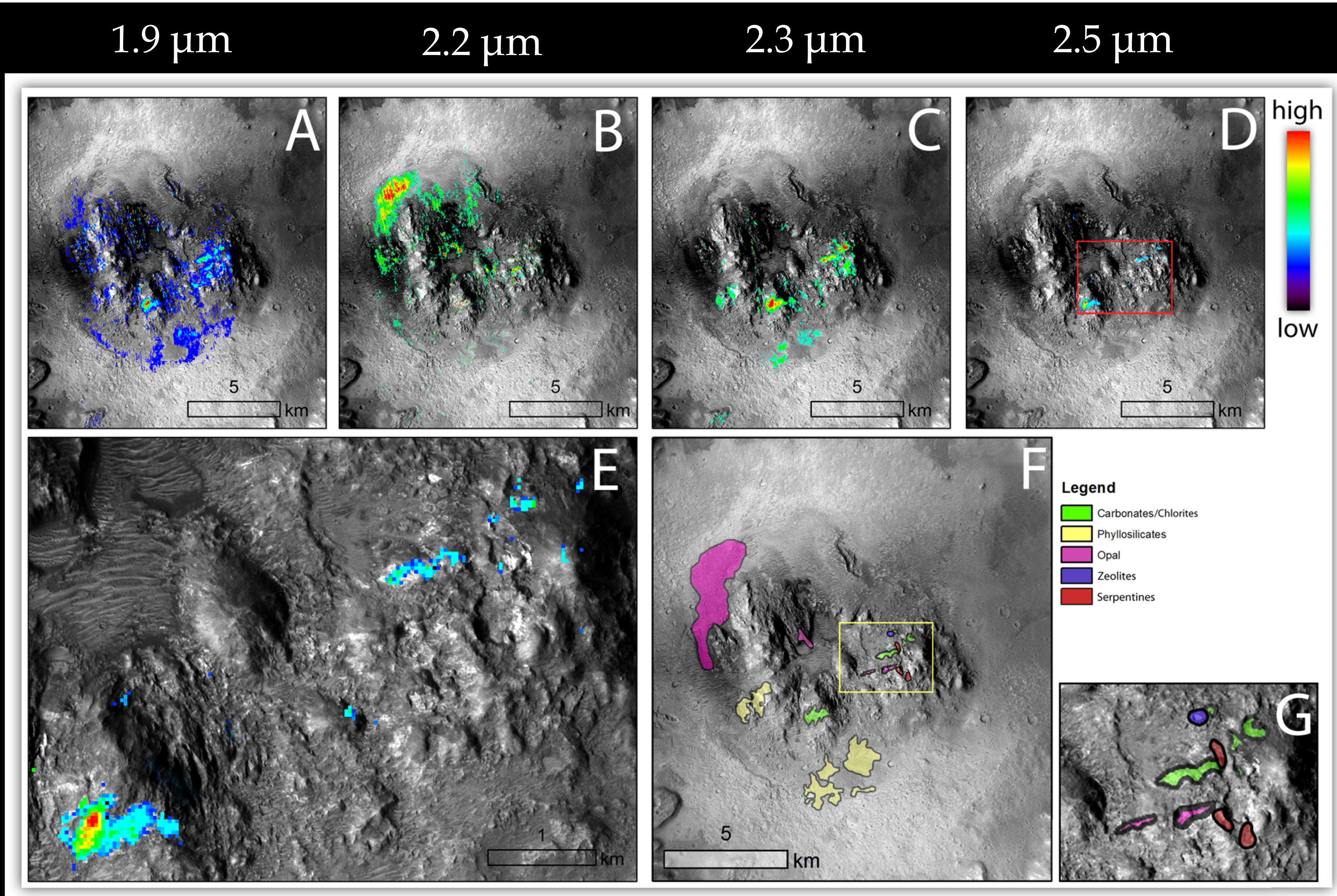

Spatial distribution of the band depth at (A) 1.9 µm used for identification of hydrated minerals (note that the NE-SW distribution of the minerals likely reflects the fracture pattern), (B) 2.2 µm for identification of silica, (C) 2.3 µm for identification of carbonates, phyllosilicates and chlorites, and (D) BDCARBO for identification of carbonates. The value ranges are 0.0 05–0.040, 0.0 07–0.020, 0.0 07–0.030 and 0.02–0.07, respectively. In panel (E) is a close-up view (see red area in the d panel for location) of the peak pit. Panel (F) shows the distribution of the most representative minerals and (G) shows a close-up of the central peak pit of panel F

CENTRAL UPLIFT

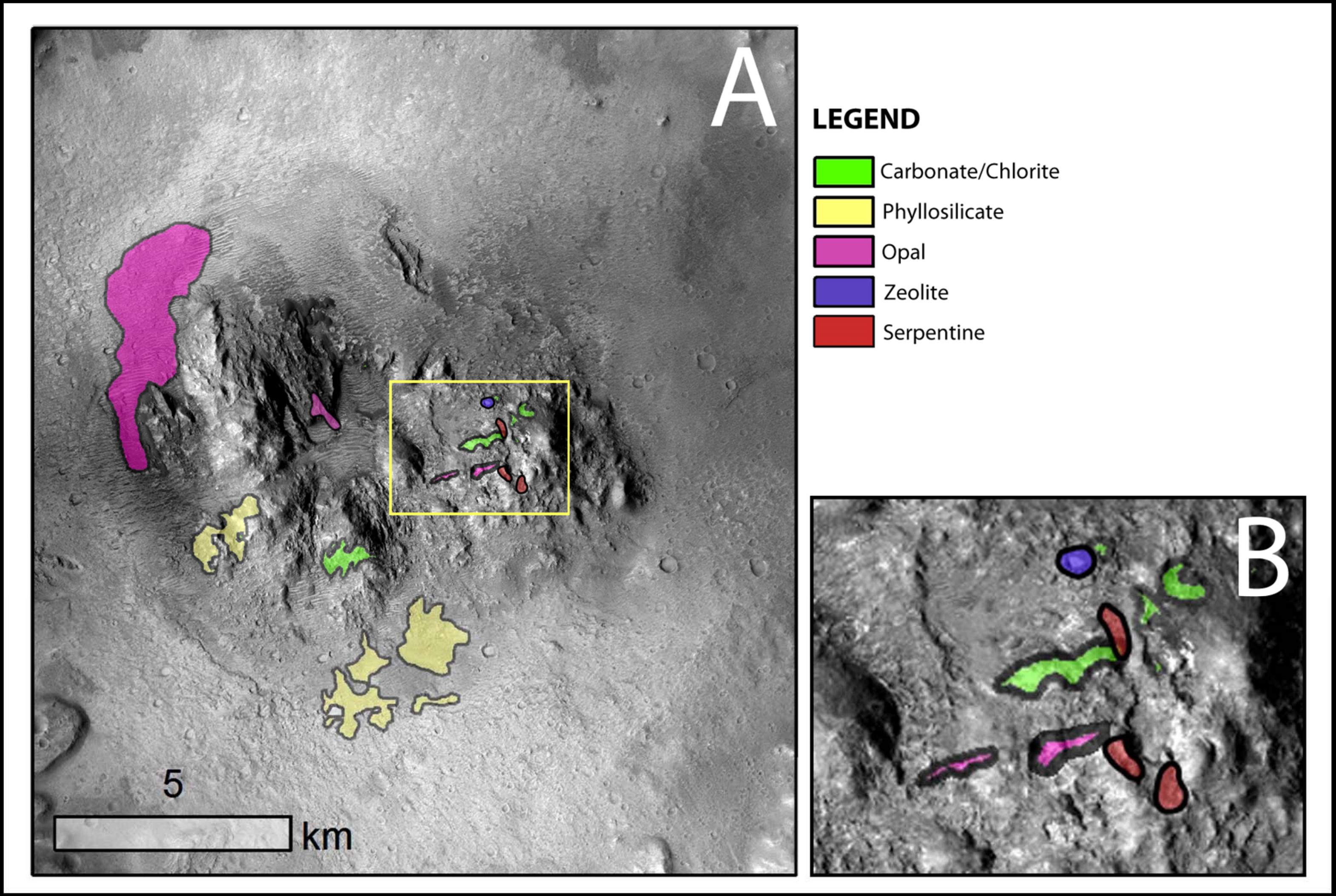

A) distribution of the most representative minerals and (B) close-up of the central peak pit of panel A.
Using the ratioed spectra we have identified various groups of minerals: phyllosilicates, carbonates, chlorites, hydrated silica, zeolites, olivines and pyroxenes.

RELATIONSHIPS BETWEEN OBSERVED MINERALS AND GEOLOGY/GEOMORPHOLOGY

HYDRATED SILICAS are observed in two units: in the central uplift and in a large area of the floor located in the northwest. They show the highest concentration of light-toned veins.

CARBONATES, SERPENTINE, ZEOLITE and CHLORITES are almost exclusively located in the hilly peak pit area.

PHYLLOSILICATES are the dominant phase and sometimes occur mixed with other phases. They have been detected in many locations of the central uplift, around its base and in other sites in association with hydrated silica and anhydrous minerals.

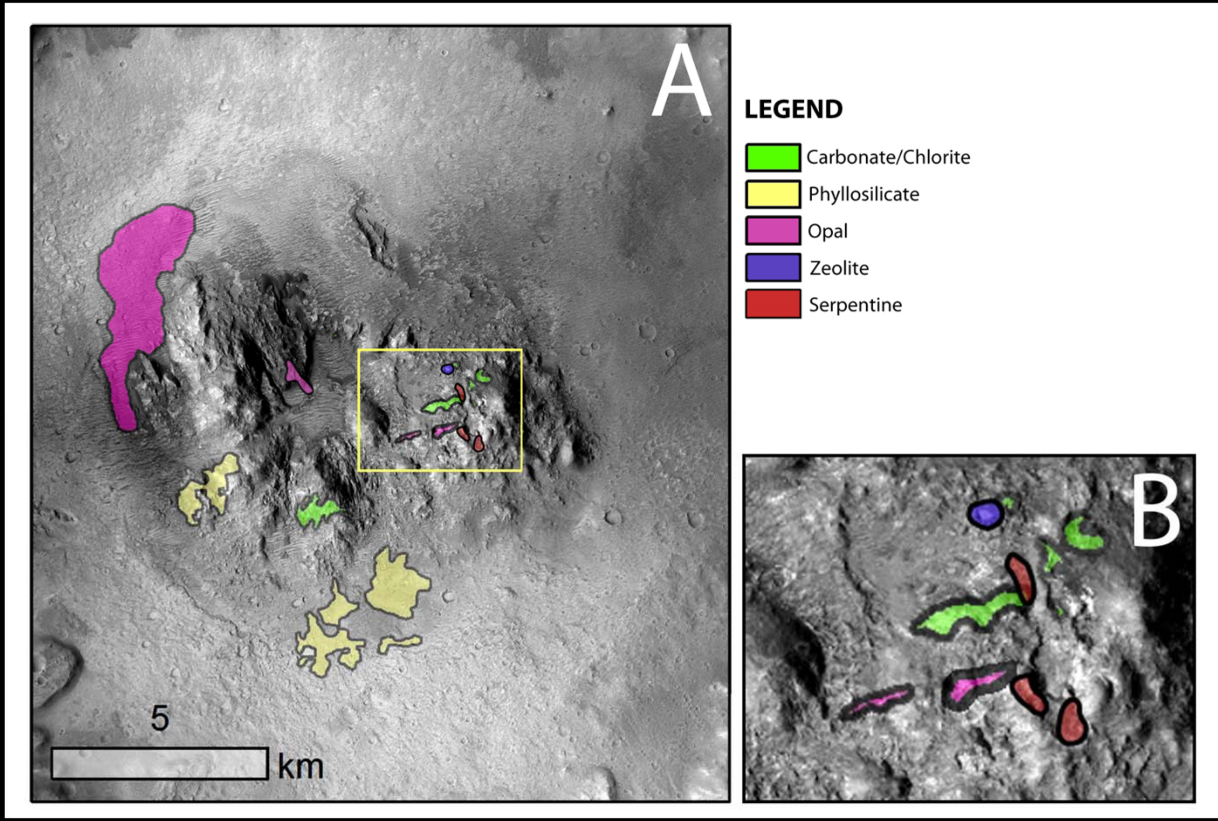

Close-up view from HiRISE images and location of the polygonal terrains:

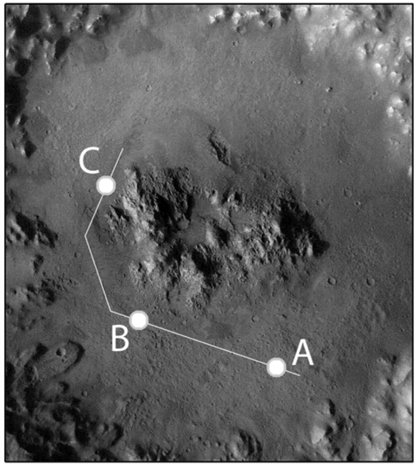

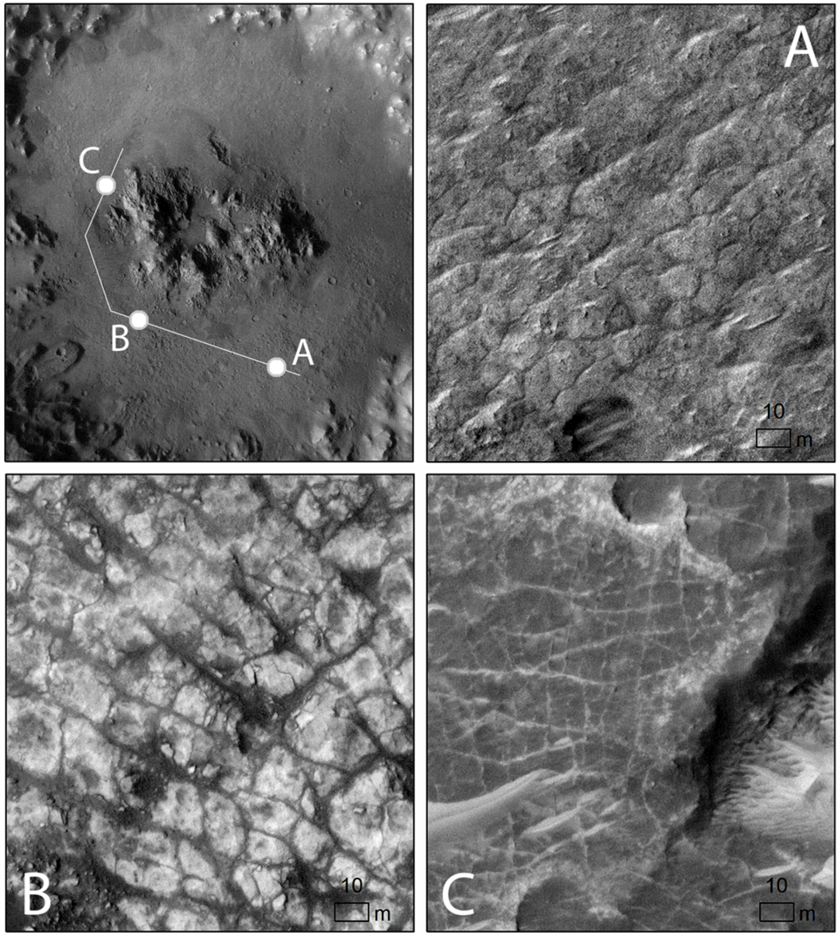

Close-up view from HiRISE images and location of the polygonal terrains: (A) honeycomb pattern, (B) polygonal cracks and bright concretional layer, (C) inverted veins polygonal network; An approximate distribution of the different polygonal terrains it is shown along the topographic profile in the bottom panel. The profile it is extracted from the line of the upper-right panel. The polygonal terrains can be divided into three main sites based on their morphology and stratigraphy.

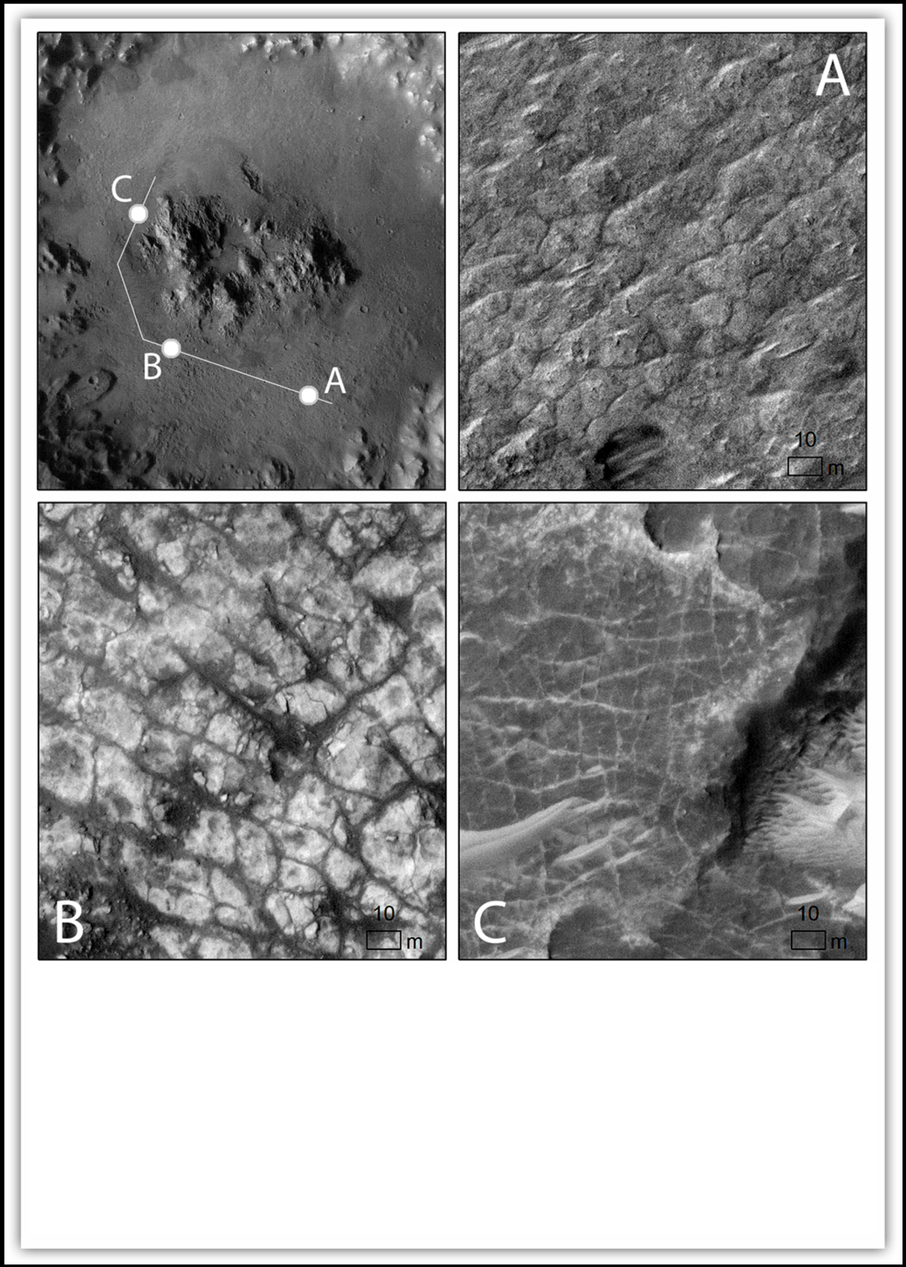

Close-up view from HiRISE images and location of the polygonal terrains: (A) honeycomb pattern, (B) polygonal cracks and bright concretional layer, (C) inverted veins polygonal network; An approximate distribution of the different polygonal terrains it is shown along the topographic profile in the bottom panel. The profile it is extracted from the line of the upper-right panel.

VEINS AND POLYGONAL TERRAINS SUGGEST THAT THE ALTERATION IS DUE TO HYDROTHERMAL CIRCULATION OF FLUIDS.

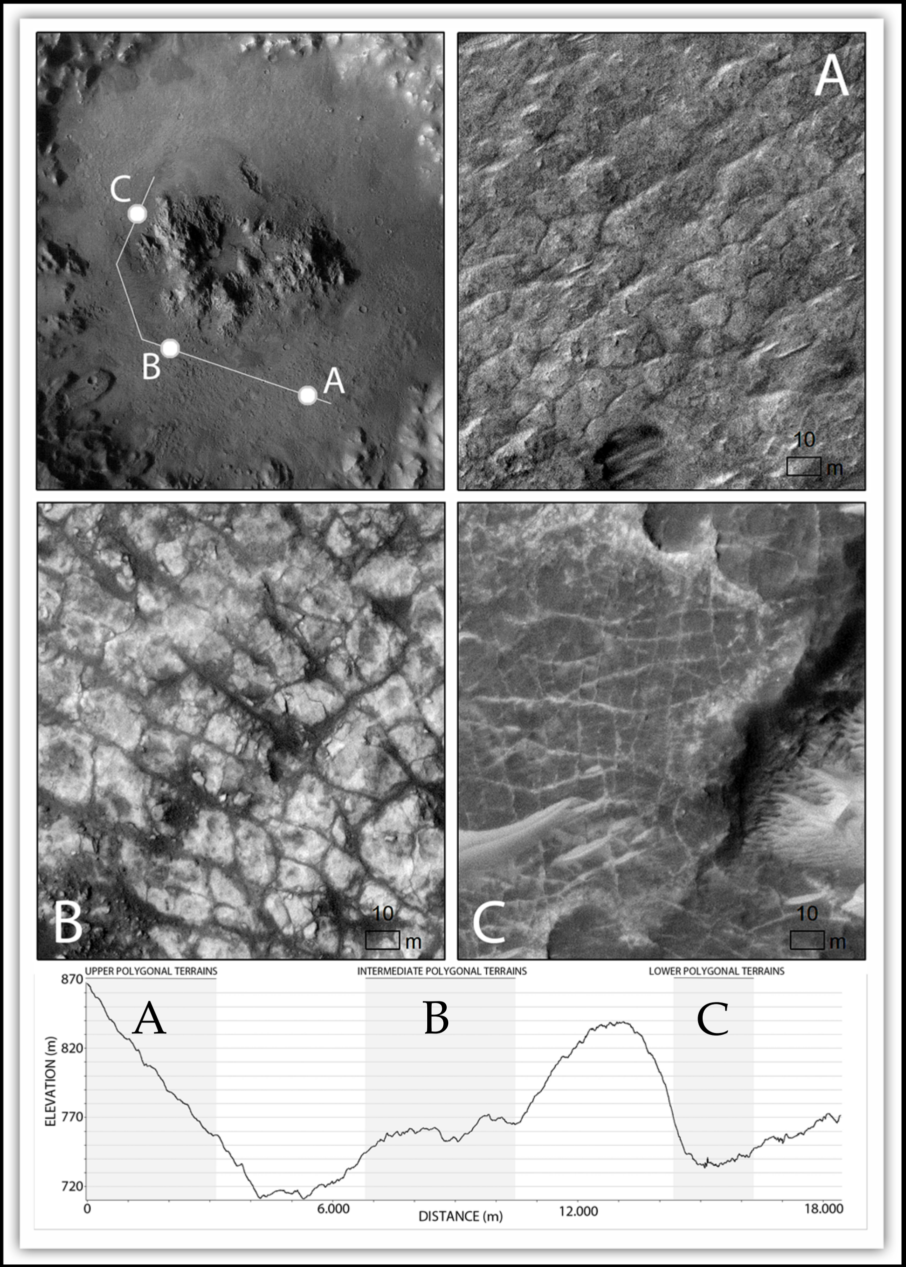

Close-up view from HiRISE images and location of the polygonal terrains: (A) honeycomb pattern, (B) polygonal cracks and bright concretional layer, (C) inverted veins polygonal network; An approximate distribution of the different polygonal terrains it is shown along the topographic profile in the bottom panel. The profile it is extracted from the line of the upper-right panel

VEINS AND POLYGONAL TERRAINS SUGGEST THAT THE ALTERATION IS DUE TO HYDROTHERMAL CIRCULATION OF FLUIDS.

The stratigraphic relationship between different mineral units is the result of different temperatures regimes within the zone of hydrothermal alteration. (C) Deepest inverted type show veins and are correlated with spectral evidence for silica, (A,B) while the intermediate and highest terrains are not affected by veins and are correlated with spectral signatures for phyllosilicates. This might be explained by the vertical zonation of the hydrothermal processes

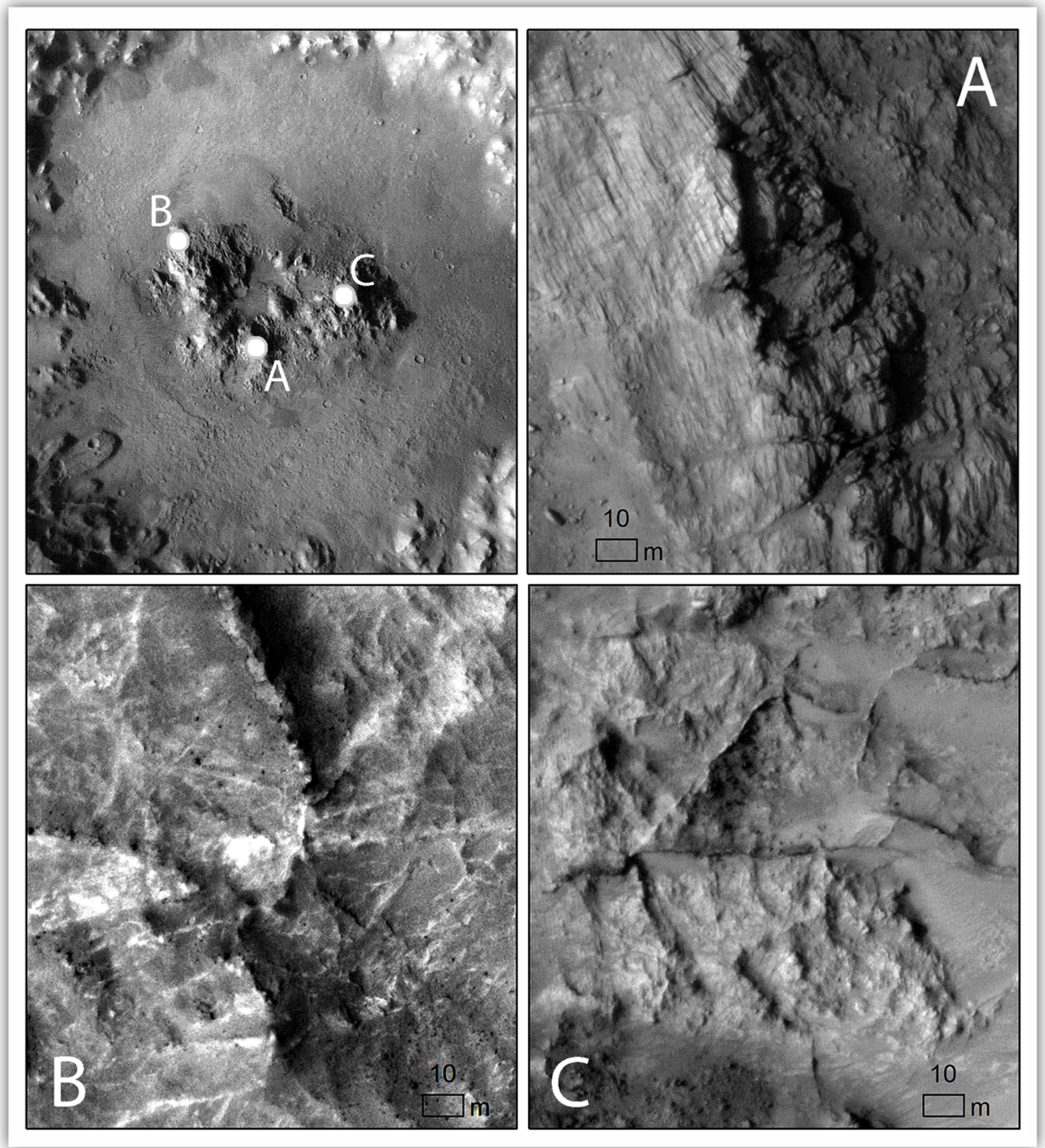

Close-up view from HiRISE images and location of the joints, fractures and veins visible on the central peak pit units: (A) fractures network on the exhumed bedrock, (B) bright veins, (C) inverted/raised dark veins/ridges. HiRISE images: ESP_020161_1640 and PSP_005683_1640, ESP_011458_1640.

MOUNDS

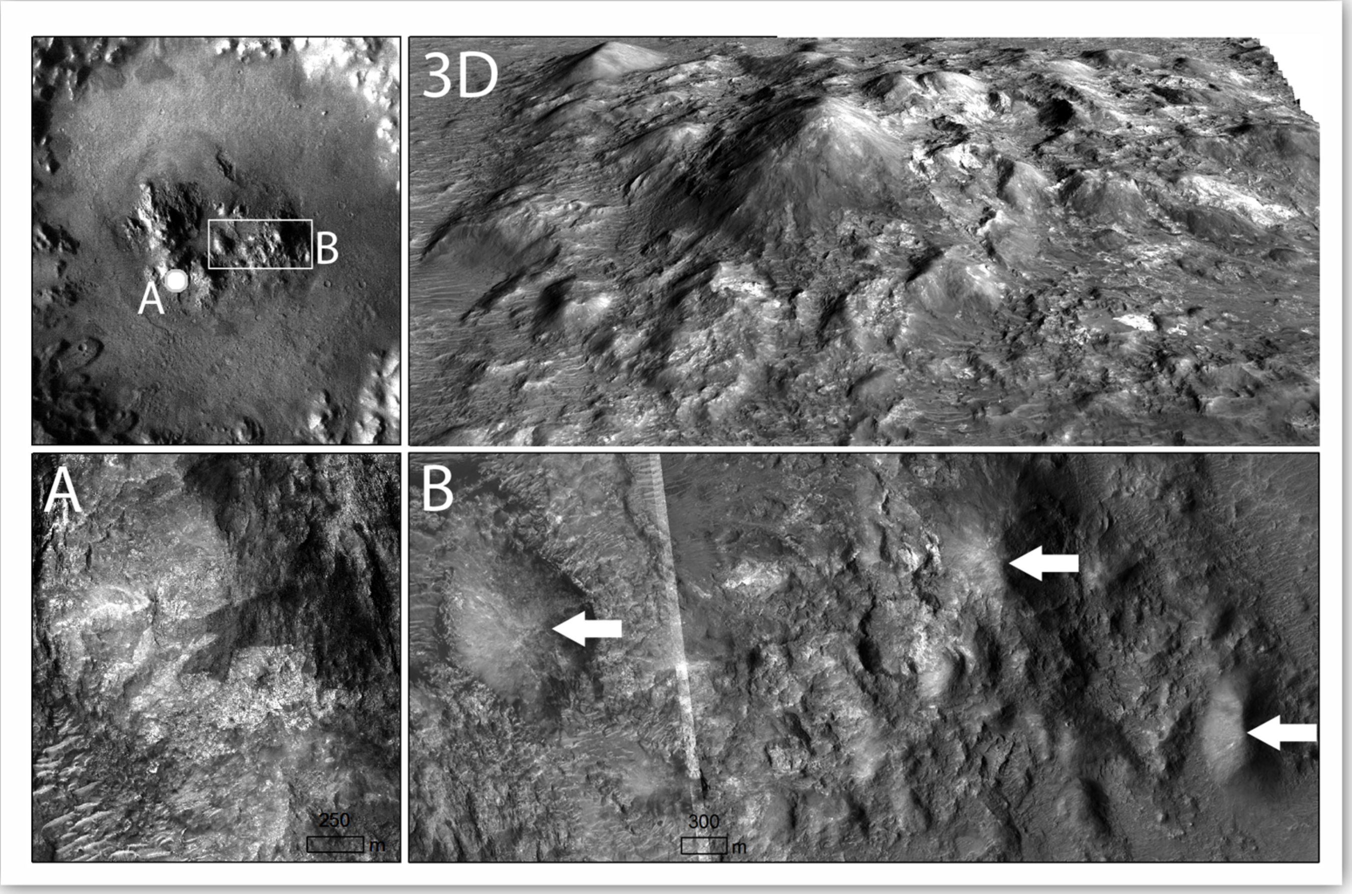

Close-up view from HiRISE images and (A) location of the bright carbonates outcrop; (B) possible spring mounds (marked by arrows) in the eastern portion of the central peak pit shown also in perspective view (realized from HiRISE stereo-derived topography) in the upper right panel.

Although there is no evidence for the depressions at the top of these latter structures to be interpreted as possible vents, the lack of depressions on the observed mounds may be explained through post-depositional erosion and/or concealment by dust deposition

SEQUENCE OF EVENTS

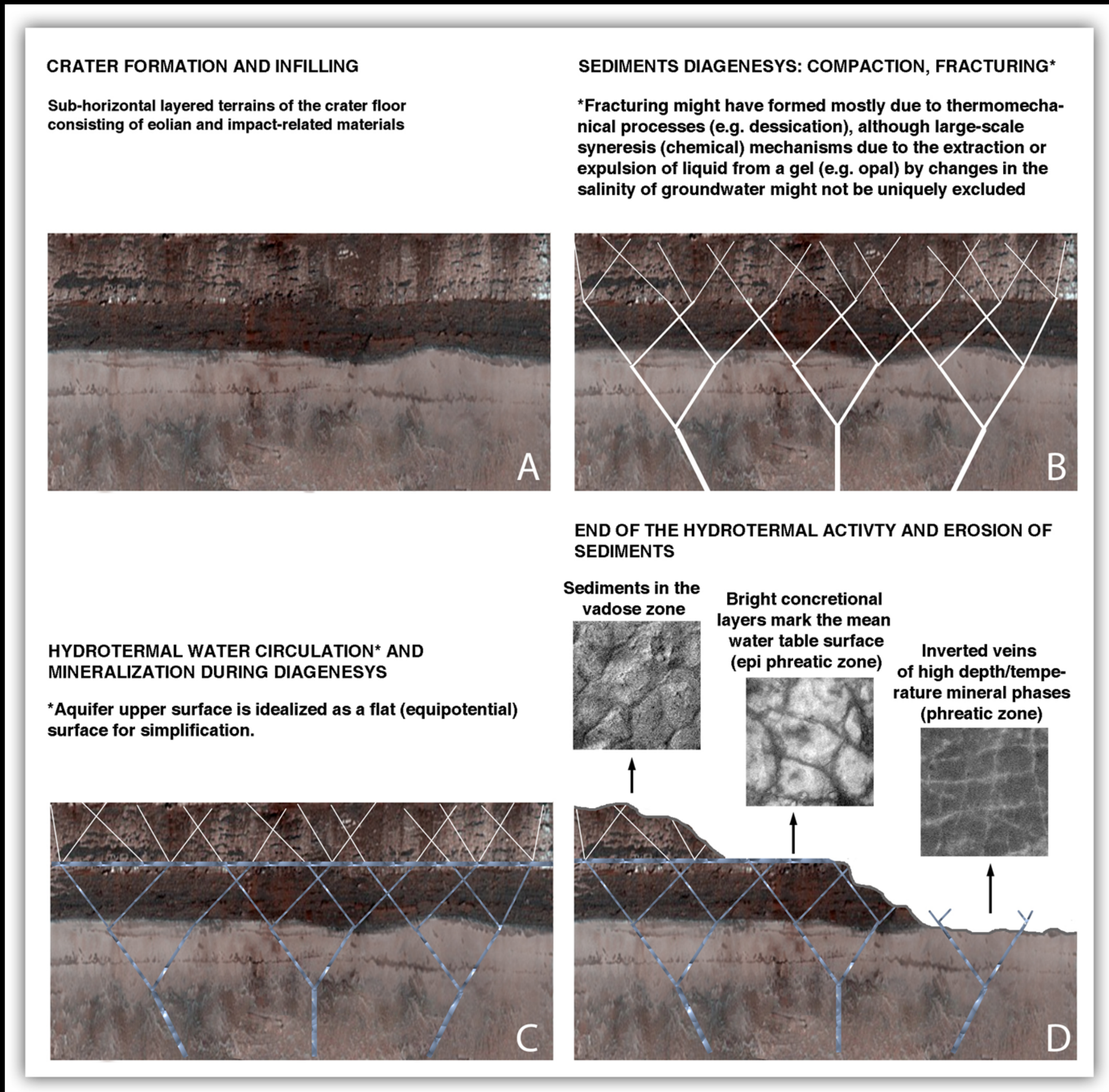

Schematic cross section representation and synthesis of processes sequence leading to the formation of the polygonal terrains characterizing the crater floor. The layers are for illustration purposes only and do not reflect the scale and the different composition of the actual stratigraphy.

The distribution of the hydrated minerals in and around the central uplift and the stratigraphic relationships of the carbonate units suggest two main mechanisms (likely partially overlapping) to explain their origin:

- crater formation and subsequent excavation and exhumation of carbonate-rich bedrock units
- impact-induced hydrothermal circulation within fractures and subsequent mineral deposition.

IN SUMMARY

The geological evolution of the studied area could be reconstructed with the crater formation, which exhumed/uplifted carbonate-rich bedrock that is visible in the crater peak pit area and activated a vertically zoned hydrothermal system. The latter system determined the alteration of mafic rocks to silica, phyllosilicates, zeolites and chlorites and likely secondary carbonate mineral phases.

IN SUMMARY

The geological evolution of the studied area could be reconstructed with the crater formation, which exhumed/uplifted carbonate-rich bedrock that is visible in the crater peak pit area and activated a vertically zoned hydrothermal system. The latter system determined the alteration of mafic rocks to silica, phyllosilicates, zeolites and chlorites and likely secondary carbonate mineral phases.

We interpreted the polygonal terrains as evidence of different preservation stages and stratigraphic exposures of the crater floor deposits sequence. Specially, the upper are interpreted as relatively pristine, the intermediate as eroded7deflated, and the lower terrains as the oldest and topographically inverted.

IN SUMMARY

The geological evolution of the studied area could be reconstructed with the crater formation, which exhumed/uplifted carbonate-rich bedrock that is visible in the crater peak pit area and activated a vertically zoned hydrothermal system. The latter system determined the alteration of mafic rocks to silica, phyllosilicates, zeolites and chlorites and likely secondary carbonate mineral phases.

We interpreted the polygonal terrains as evidence of different preservation stages and stratigraphic exposures of the crater floor deposits sequence. Specially, the upper are interpreted as relatively pristine, the intermediate as eroded7deflated, and the lower terrains as the oldest and topographically inverted.

Given the lack of any signs of hydrological activity from the inner crater rim slope such as valley networks, it can be concluded that the water for the hydrothermal system was provided by underground circulation and/or melting of water ice.

IN SUMMARY

The geological evolution of the studied area could be reconstructed with the crater formation, which exhumed/uplifted carbonate-rich bedrock that is visible in the crater peak pit area and activated a vertically zoned hydrothermal system. The latter system determined the alteration of mafic rocks to silica, phyllosilicates, zeolites and chlorites and likely secondary carbonate mineral phases.

We interpreted the polygonal terrains as evidence of different preservation stages and stratigraphic exposures of the crater floor deposits sequence. Specially, the upper are interpreted as relatively pristine, the intermediate as eroded7deflated, and the lower terrains as the oldest and topographically inverted.

Given the lack of any signs of hydrological activity from the inner crater rim slope such as valley networks, it can be concluded that the water for the hydrothermal system was provided by underground circulation and/or melting of water ice.

If the hydrothermal activity occurred, it was not restricted to the central uplift but was also present in the crater cavity.

IN SUMMARY

The geological evolution of the studied area could be reconstructed with the crater formation, which exhumed/uplifted carbonate-rich bedrock that is visible in the crater peak pit area and activated a vertically zoned hydrothermal system. The latter system determined the alteration of mafic rocks to silica, phyllosilicates, zeolites and chlorites and likely secondary carbonate mineral phases.

We interpreted the polygonal terrains as evidence of different preservation stages and stratigraphic exposures of the crater floor deposits sequence. Specially, the upper are interpreted as relatively pristine, the intermediate as eroded7deflated, and the lower terrains as the oldest and topographically inverted.

Given the lack of any signs of hydrological activity from the inner crater rim slope such as valley networks, it can be concluded that the water for the hydrothermal system was provided by underground circulation and/or melting of water ice.

If the hydrothermal activity occurred, it was not restricted to the central uplift but was also present in the crater cavity.

The strong correlation between the observed minerals (carbonate, opaline, smectite, chlorite, serpentine and zeolite) and morphology (veins, polygonal terrains and mounds) of hydrothermal origin makes the studied crater one of the best candidates for hosting an ancient post-impact hydrothermal system.

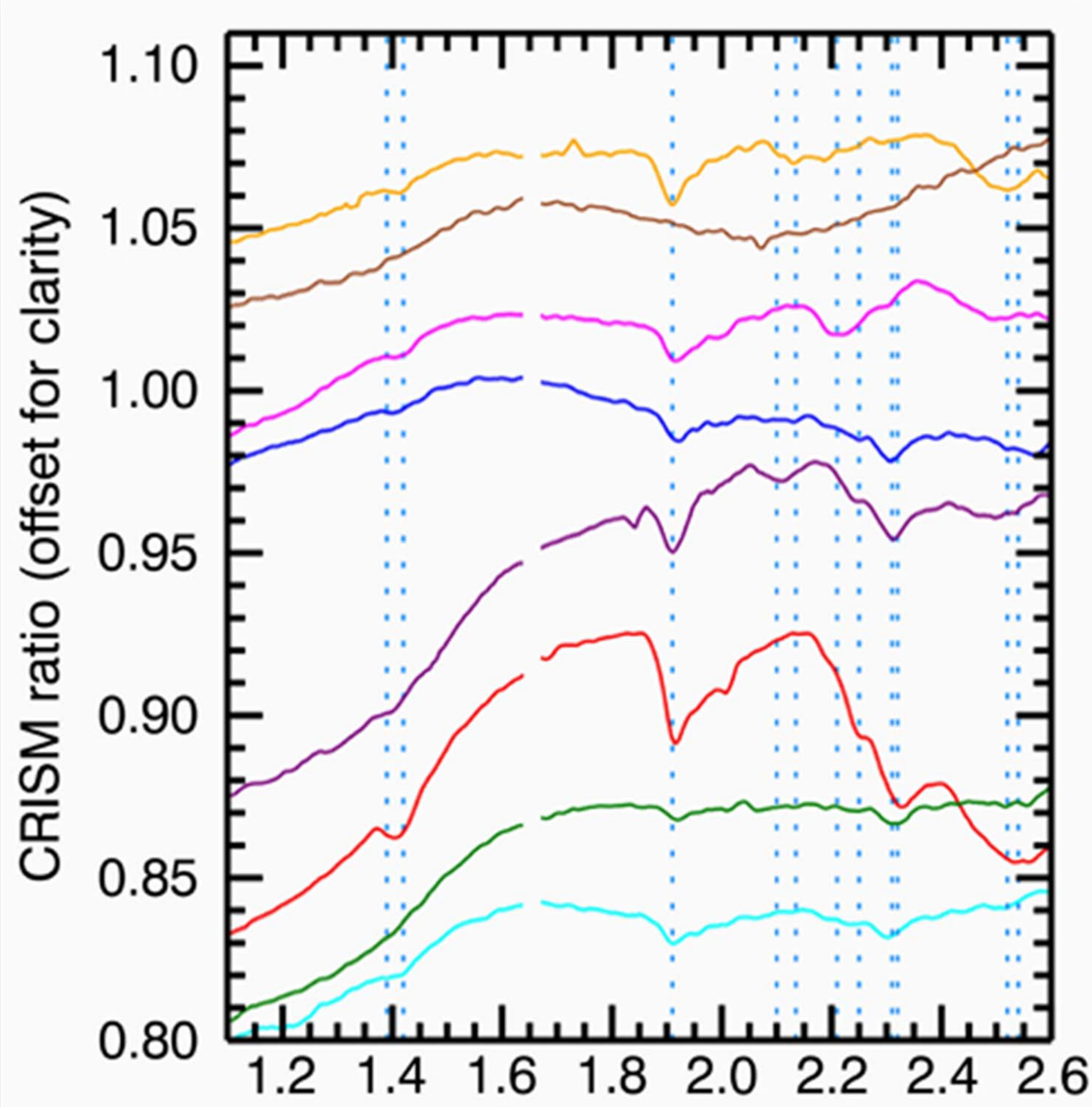
CRISM ratio (offset for clarity)
1.10
1.05
1.00
0.95
0.90
0.85
0.80
1.2
1.4
1.6
1.8
2.0
2.2
2.4
2.6

SCHEMATIC CROSS SECTION OF A COMPLEX CRATER

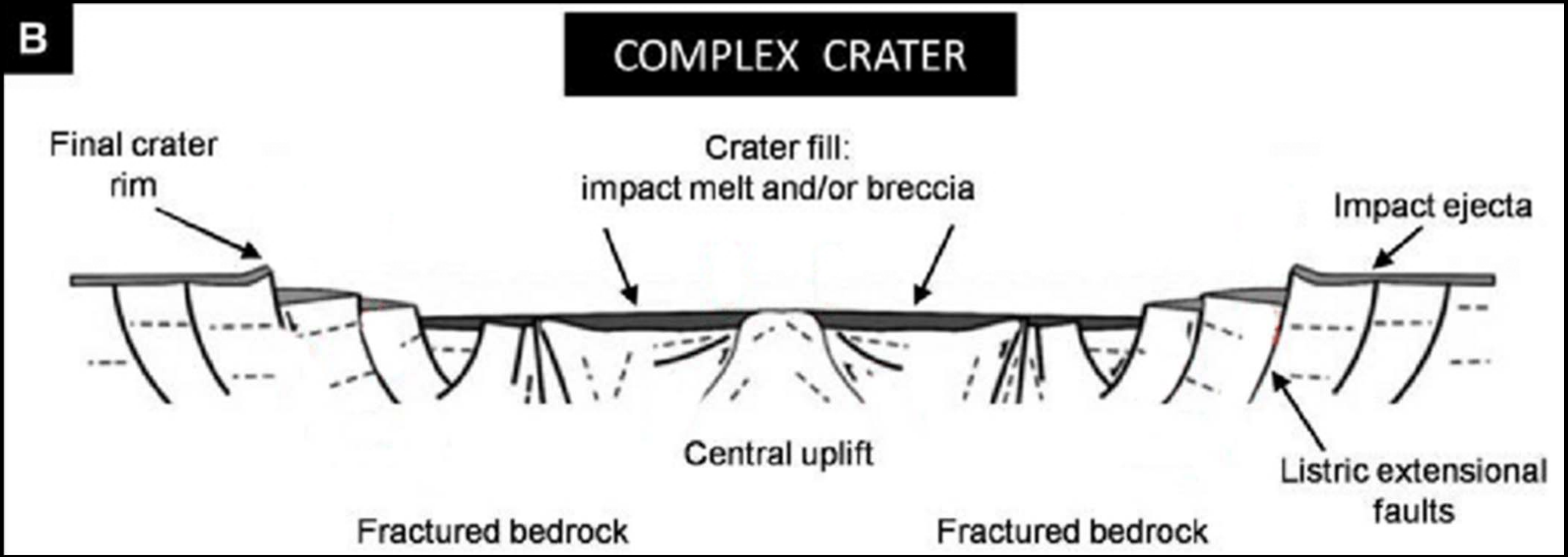

Schematic cross sections of impact craters. These illustrate potential CH 4 generated at depth (by any process) and subsequent fluid flow (arrows) through fractures, faults, and unconformity surfaces. Complex crater, adapted from Melosh (1989) and Osinski et al. (2005); dashed arrow indicates potential CH 4 release associated with central uplifts

SCHEMATIC CROSS SECTION OF A COMPLEX CRATER

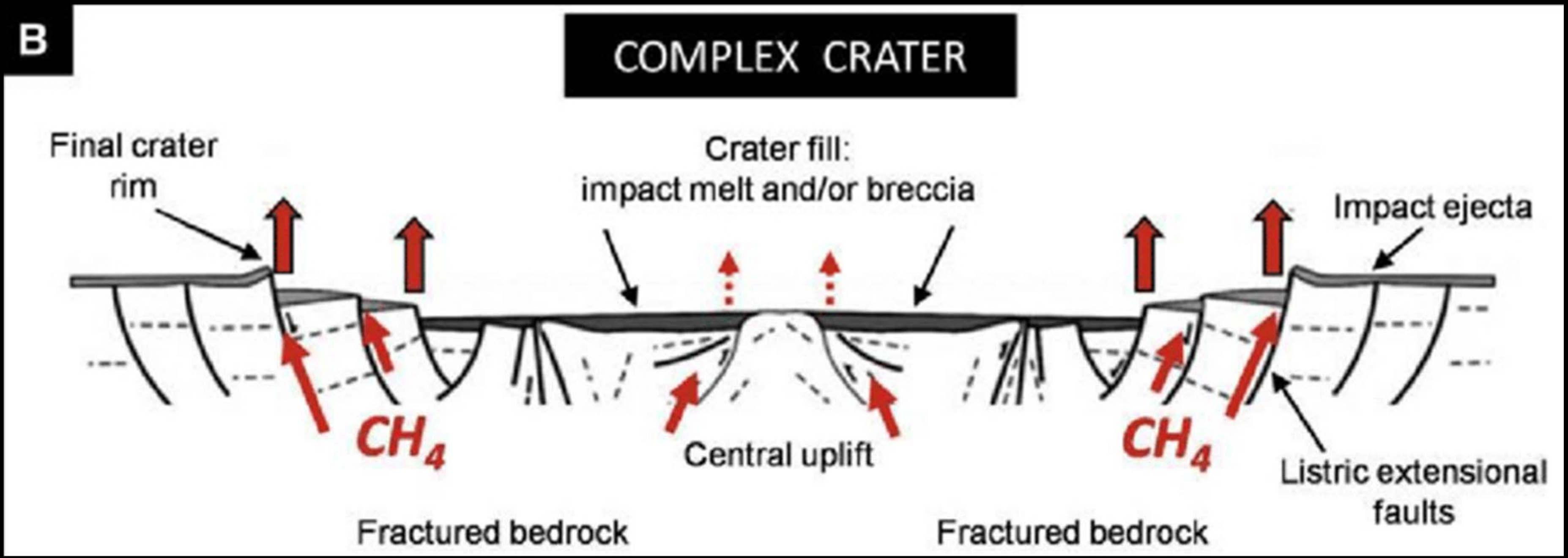

Schematic cross sections of impact craters. These illustrate potential CH 4 generated at depth (by any process) and subsequent fluid flow (arrows) through fractures, faults, and unconformity surfaces. Complex crater, adapted from Melosh (1989) and Osinski et al. (2005); dashed arrow indicates potential CH 4 release associated with central uplifts